HAL open science

Biopolymer Blends Based on Poly (lactic acid): Shear and Elongation Rheology/Structure/Blowing Process Relationships

Racha Al-Itry, Khalid Lamnawar, Abderrahim Maazouz

▶ **To cite this version:**

Racha Al-Itry, Khalid Lamnawar, Abderrahim Maazouz. Biopolymer Blends Based on Poly (lactic acid): Shear and Elongation Rheology/Structure/Blowing Process Relationships. Polymers, 2015, 7 (939-962), ⟨10.3390/polym7050939⟩. ⟨hal-01151959⟩

HAL Id: hal-01151959

https://hal.science/hal-01151959v1

Submitted on 26 Feb 2025

HAL is a multi-disciplinary open access archive for the deposit and dissemination of scientific research documents, whether they are published or not. The documents may come from teaching and research institutions in France or abroad, or from public or private research centers.

L'archive ouverte pluridisciplinaire **HAL**, est destinée au dépôt et à la diffusion de documents scientifiques de niveau recherche, publiés ou non, émanant des établissements d'enseignement et de recherche français ou étrangers, des laboratoires publics ou privés.

Autorisation HAL

HAL Authorization

Polymers **2015**, *7*, 939-962; doi:10.3390/polym7050939

OPEN ACCESS

polymers

ISSN 2073-4360

www.mdpi.com/journal/polymers

Article

Biopolymer Blends Based on Poly (lactic acid): Shear and Elongation Rheology/Structure/Blowing Process Relationships

Racha Al-Itry [1,2], Khalid Lamnawar [1,3] and Abderrahim Maazouz [1,2,4,*]

[1] Institut National des Sciences Appliquées (INSA), Université de Lyon, Lyon F-69361, France; E-Mails: Racha.Al-Itry@insa-lyon.fr (R.A.-I.); khalid.lamnawar@insa-lyon.fr (K.L.); abderrahim.maazouz@insa-lyon.fr (A.M.)

[2] UMR (Unité Mixte de Recherche) 5223, Ingénierie des Matériaux Polymères IMP, Centre National de la Recherche Scientifique (CNRS), INSA Lyon, Villeurbanne F-69621, France

[3] UMR (Unité Mixte de Recherche) 5259, Laboratoire de Mécanique des Contacts et des Structures LaMCoS, Centre National de la Recherche Scientifique (CNRS), INSA Lyon, Villeurbanne F69621, France

[4] Hassan II Academy of Science and Technology, Rabat, Morocco

* Author to whom correspondence should be addressed; E-Mail: abderrahim.maazouz@insa-lyon.fr; Tel.: +33-472-436-332; Fax: +33-472-438-515.

Academic Editor: Patrick Ilg

Received: 18 March 2015 / Accepted: 29 April 2015 / Published: 13 May 2015

Abstract: This study was dedicated to the blown film extrusion of poly(lactic acid), which mainly presents poor shear and elongation viscosities, and its blends. In order to enhance its melt strength, two main routes were selected (i) a structural modification through chain extension and branching mechanisms by adding a reactive multifunctional epoxide (named Joncryl) and (ii) blending with poly(butylene adipate-*co*-terephtalate), named PBAT in presence (or not) of Joncryl. The effects of the reactive agent on the shear and elongation rheology, morphological, and interfacial properties of the blends were systematically investigated. A decrease of the interfacial tension has been also demonstrated according to the deformed drop retraction method (DDRM). Hence, the role of Joncryl as a compatibilizer was highlighted. Consequently, finer morphology of the dispersed phase was obtained. Furthermore, the impact of the two modification routes on the blown film extrusion ability of PLA has been studied. Based on the improved shear and elongational rheological properties, a great enlargement of the blowing processing window of PLA modified with Joncryl was demonstrated. Indeed, with the addition of Joncryl into

PLA–PBAT blends, a reduction of the instability defects has been detected. Finally, the induced crystalline structure and the thermo-mechanical properties of blown films were shown to be improved.

Keywords: biopolymers; shear and elongation rheology; structural modification; blown film extrusion; crystallization; thermo-mechanical behavior

1. Introduction

In packaging applications, the blown film extrusion represents an efficient way to make films with thin thickness and the polymer needs to possess relatively high melt strength [1,2]. Unfortunately, compared to polyolefins, poly(lactic-acid) (PLA) is typically a linear polymer with a rather low molecular weight distribution [3]. PLA rheology is not well suited for the blowing extrusion because it has relatively low melt strength, resulted from its thermal, oxidative and hydrolytic degradations [4,5]. These degenerative effects lead, during processing, to the cleavage of the polymer manifested by a loss of the molecular weight and deterioration of rheological properties when higher shear and extensional deformations are required in such process [6]. Another shortcoming of PLA is its brittle properties. PLA should be therefore melt strengthened under processing. Many strategies have motivated considerable research efforts. In particular, two strategies are presented here: (i) modification of PLA through branched architecture with chain-extension reactions to compensate for the molecular weight decrease caused by the processing degradation [7,8] and (ii) blending PLA with other natural or synthetic materials such as Polycaprolacton (PCL), starch, poly (butylene adipate-*co*-terephtalate) (PBAT), poly(butylene succinate-*co*-adipate) (PBSA), *etc*. [9].

A better understanding of the blowing extrusion process is still of high actuality. Rheological measurements, in shear and in elongation flows, should be well established to characterize polymers with respect to processing. Extensional flow of polymer melts is a more challenging task in comparison to the shearing deformations. The subtle changes in molecular architecture are readily detected in the processing performance of PLA and more readily visible in extensional deformations [10].

On the one hand, the chemical chain extension of PLA using a chain extender is highly discussed. Some experiments have been conducted by our team researchers in previous works [5–9,11–13]. We showed that the structural modification of PLA highly increased the shear rheological properties (melt strength, zero-shear viscosity, elasticity, shear-thinning behavior) and contributed to very long relaxation process. A complex structure *i.e*., mixture of linear and randomly branched chains, was deduced according to Van–Gurp–Palmen plots, molar measurements and viscometric properties. During elongation, linear PLA does not exhibit any strain-hardening. This was due to linear chains being free from any branch points and was not prevented from slipping over each other. Several modification routes have been discussed in the literature in order to create a strain-hardening. Liu *et al*. [14] found that the strain hardening was not observed in PLA without long chain branches (LCB) or even in the PLA with star branched structure. Palade *et al*. [15] reported that the presence of a low fraction of high molecular of PLA makes the strain-hardening occurred. Yamane *et al*., showed that the addition of small amounts of poly(D,L-lactic acid) (PDLA) into PLLA could lead to strain-hardening in poly(L-lactic acid) (PLLA)

melts due to the stereocomplex formation acting as branching points on the PLA chains. The effects of chain branching of PLA on foaming ability have been investigated by extensional flow experiment [14,16,17]. The authors found that the chemical chain-extension enhanced the extensional flow of PLA where a relevant strain hardening appeared due to the presence of long chain branches when the macromolecular chain disentanglement rate is too low in relation with the deformation rate. This resistance to stretching became stronger as the chain extender content was increased. Additionally, the presence of LCB in PLA has shown the relationship between the extension rate and the extent of strain hardening, namely that strain hardening occurred faster at higher extension rates. Moreover, the extensional rheological experimental results of branched PLAs elucidated that the LCB–PLA has shown the foaming process-ability with fine cell structures. However, they reported that some processing limitations arose at a very high extension ratio (a high content of chain extender) because of the high melt elasticity. Meanwhile, Mallet *et al.* [13] discussed the improved elongational properties and the stability blowing extrusion properties of modified PLA using a ternary system (chain-extenders, plasticizers and nucleating agents).

On the other hand, blending PLA with PBAT presents a suitable approach to improve its mechanical properties. In our previous work [5], we have reported an improvement of the elongation at break and toughness of PLA–PBAT blends even at low concentrations of PBAT. The effect of the chain extension reaction on the interfacial properties of PLA–PBAT blends has been also studied [9]. However, few works have been dedicated to study the elongational behavior of blends based on PLA in the molten state. Eslami *et al*. [18] evaluated the elongational rheology of PLA/PBSA blends with different blend compositions. They found that PLA/ PBSA blends containing less than 50 wt% PBSA showed no clear strain-hardening behavior. However, a well-defined strain hardening behavior was observed for blends containing PBSA at concentrations of 50 wt% or higher.

Compared to polyethylene [19,20], literature works covering molecular characterization, elongational rheology and film blowing are very rare. That is why new insight can be expected from the results reported in this paper.

The ultimate objective of the present work is thus dedicated to the film blowing process for PLA and its blends. It deals with the better understanding of the structure modification and compatibilization on the physical and morphological properties of PLA–PBAT blends, with special emphasis on their elongational rheology. A clear correlation between the induced shear and elongation properties on the blown extrusion stability process has been also discussed. The micro-structural and thermo-mechanical properties of the blown biopolymer films have been finally investigated.

2. Experimental Section

2.1. Polymers Used

PLA (Grade: 4032D) with a weight- average molar weight of 100.000 g/mol (Gel Permeation Chromatography GPC analysis), was purchased from Natureworks (Minnetonka, MN, USA), and consisted of 2% D-Lactide units. PBAT (Grade: Ecoflex FBX 7011) was obtained from BASF (Ludwigshafen, Germany). It exhibits a weight-average molar weight of 40.000 g/mol (GPC analysis), a glass transition temperature and melting point of −30 °C and 110–120 °C (Differential Scanning

calorimetry DSC analysis), respectively. Commercial multi-functional styrene-acrylic oligomers (BASF, Joncryl ADR®-4368) accepted by the Food & Drug Administration (FDA) for food packaging, were used. It is an epoxy functional oligomeric acrylic with the following physical characteristics: Transition temperature T_g = 54 °C, EEW (epoxy equivalent weight) = 285 g/mol, M_w = 6800 g/mol, obtained in flake form. Table 1 summarizes the compositions of the various studied samples.

Table 1. Composition of the different studied samples.

Notations	Composition
PLA	100 wt% PLA
PBAT	100 wt% PBAT
PLA-0.7	99.3 wt% PLA + 0.7 wt% Joncryl
PBAT-0.7	99.3 wt% PBAT + 0.7 wt% Joncryl
80–20	80 wt% PLA + 20 wt% PBAT
80–20–0.25	79.8 wt% PLA+ 19.95 wt% PBAT + 0.25 wt% Joncryl
80–20–0.5	79.6 wt% PLA + 19.9 wt% PBAT + 0.5 wt% Joncryl
80–20–0.7	79.44 wt% PLA + 19.86 wt% PBAT + 0.7 wt% Joncryl
80–20–1	79.2 wt% PLA + 19.8 wt% PBAT + 1 wt% Joncryl

2.2. Sample Preparation and Preliminary Work

2.2.1. Blends Preparation

Before compounding, both PBAT and PLA pellets were dried under vacuum at 80 °C for 12 h to remove moisture. Joncryl ADR® was also dried under vacuum at 60 °C. Numerous papers have been published by our research group on the reactivity of Joncryl on both PLA and PBAT polymers [5,11–13]. Since its higher functionality, Joncryl reacts via its epoxy rings with carboxyl and hydroxyl groups of both polyesters.

The preparation of samples was carried out under nitrogen flow in a corotating twin-screw extruder having a clam shell barrel design with a length:diameter ratio of 25:1 (Thermo Electron Polylab System Rhecord RC400P, Courtaboeuf, France). The screw rotation speed was set at 40 rpm during 3 min. The temperature profile was set at 140 °C (feeding zone), 190 °C, 180 °C (melting zones) and 180 °C (die). After melt blending, each extrudate was quenched in a cold water bath and granulated. A special sealed and heated hopper was used. The twin screw profile was optimized to obtain good dispersion properties. For the sake of clarity, only the results of the modified polymers and blends at the end of the reaction were studied here, for which the viscoelastic parameters (complex viscosity and storage modulus) remain unchanged during time.

2.2.2. Validation of Reaction Completion with Multifunctional Epoxide

The optimal reaction times with Joncryl were evaluated based on the monitoring of the experimental *in situ* stabilization of the torque *versus* time to be sure that the samples are not changing in time and no thermal degradation can occur. Moreover, the samples stability with time was studied during a dynamic time sweep test (DTS) by plotting the normalized complex viscosity modulus $\eta^*(t)/\eta(t = 0)$ *versus* time at various temperatures ranging from 180 to 200 °C and the rheo-kinetic properties

as well the apparent conversion and the end reaction time are determined. In a previous work [5], the stabilization region was thus determined when achieving a viscosity plateau *i.e.*, when the reaction between PLA (or PBAT) with chain extender has finished. We have previously concluded that for the modified PLA with less than 0.7% of multi-functionalized epoxy, 3 min are quite sufficient with 180 °C. With higher Joncryl amount, the reaction need longer time (higher than 10 min) to be stabilized. Therefore, the compounds with 1% of Joncryl were re-granulated and passed once again in the twin screw extruder until achieving a stable torque.

2.2.3. Blown Film Extrusion

Blowing extrusion was performed using and annular 25 mm diameter blow die coupled to a melt pump and twin—extruder to process the PLA, PBAT and their blends into a tubular shape. The molten polymer, in the form of a tube, exiting from the die (T^0_{die} = 180 °C) is drawn upward by a take-up device. When the process starts up, the air is introduced at the bottom of the die to inflate the tube and form a bubble. The size of the bubble is maintained at a certain internal pressure. The tube is then flattened in the nip rolls and taken up by the winder. An air ring is also used to rapidly cool the hot bubble and solidify it at some distance above the die exit. This distance is usually called Frost Line Height (FLH). The film dimensions are determined by the blow-up ratio (BUR) and the take-up ratio (TUR) (*cf.* Figure 1). BUR is defined as the ratio of the final bubble diameter (D_f) to die diameter (D_0) and is controlled by varying the air pressure; TUR is defined as the ratio of the speed of the take-up device (V_f) to the extruded material velocity (V_0) at the die exit. These two key parameters will be useful to plot the stability map (BUR *vs.* TUR).

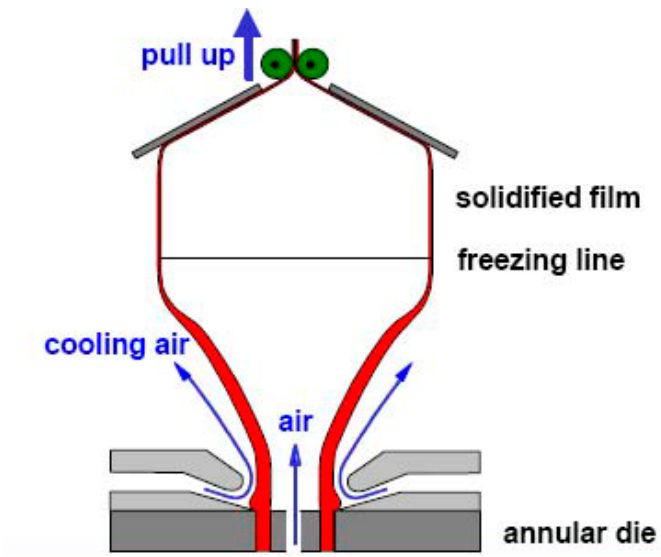

Figure 1. Schematic diagram of the film blowing experimental set-up.

2.3. Interfacial Tension Measurements

The effect of the multifunctional epoxide on the interfacial tension of the PLA–PBAT blends was determined with the deformed drop retraction method (DDRM).

DDRM-sandwich preparation: Molten polymer droplets are obtained from finely grinding powder and dispersed between two circular matrix films to form a sandwich, as presented in Figure 2. The thickness of these films is about 500 µm to 1 mm. The prepared sandwich is then heated up to the molten state of the both dispersed phase and matrix. The preparation of our sample for the measurement of interfacial tension is described schematically:

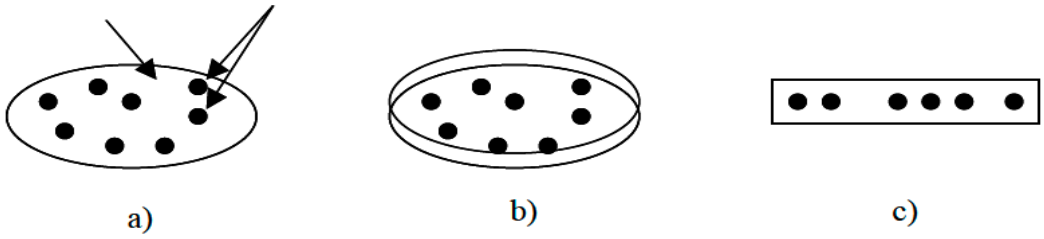

Figure 2. Three steps of sandwich preparation for the DDRM.

Step (a) consists in depositing homogeneously the dispersed phase in the form of powder over the entire surface of a matrix disk. In step (b), a second disk covers the inclusions. The sample sandwich is then introduced in the shear plate and heated (Step c); so that the inclusion and the matrix are melted. Step strain with and relaxation experiments were then performed by the Linkam device® (Surrey, UK). In order to obtain well-defined spherical droplets, the dispersed particles were subjected to a shear treatment for a few seconds (30 s; steady shear ranging from 0.1 to 5 s^{-1} for various model systems in the Newtonian rheological zone) at 180 °C. According to the higher capillary numbers, the drop first deforms into a long fibril and then breaks up into a large number of droplets through Rayleigh capillary instabilities. The sheared droplets were observed during their relaxation process through two holes made in the heating plates using a camera.

Here, we present the various experimental sandwiches (droplet/matrix):

- Model A: it is used as a reference where neat PBAT is dispersed into PLA matrix;
- Model B: it represents the more complicated systems where Joncryl reacts with both PLA and PBAT at the same time.

More details about the calculation of the interfacial tension according to DDRM carried out with the other model sandwiches were given in our previous work [9].

2.4. Morphological Study

To investigate the morphology of the blends, scanning electron microscopy (SEM) and transmission electron microscopy (TEM) were carried out. For the SEM micrographs, the cryo-fractured specimens were coated with a thin gold layer to improve the sample conductivity for observation. They were then scanned under an accelerating voltage of 8 kV. Image analysis was successfully performed on the obtained micrographs. For the TEM investigations, the microtomed specimens were stained by ruthenium tetraoxide (RuO_4) vapor for 30 min before observations.

2.5. Shear and Elongation Rheological Properties

2.5.1. Small-Amplitude Oscillatory Shear (SAOS) Measurements

The measurements were investigated with a stress-controlled rotational rheometer TA Instruments (Guyancourt, France) DHR-2 with a parallel plate geometry. The linear domain, performed at 0.1 rad/s, extends from 0.2 to 1000 Pa. During the rheological experiments, the heated chamber was continuously purged with nitrogen to avoid the potential degradation and oxidation of the polymers. Dynamic frequency sweep tests were performed at 20 Pa over an angular frequency range of 10^{-3}–628 rad/s.

2.5.2. Capillary Flow Rheology

Experimental runs with a non-isothermal flow were performed by using a pressure—controlled CEAST (Compagnia Europea Apparecchi Scientifici, Torino) capillary rheometer at 180 °C through a die with a 180° entry angle and various Length/Diameter (L/D) atios (30–20 and 5) to obtain Bagley corrections. The capillary measurements were conducted in a closed environment under nitrogen atmosphere. For this kind of experiments, the elongation viscosity was determined using Cogswell model [21].

2.5.3. Uniaxial Elongational Measurements

Experiments in uniaxial extension flow were performed using a second generation SER-2 (Sentmanat Extensional Rheometer Universal Testing Platform from Xpansion Instruments, Tallmadge, OH, USA) mounted on the DHR-2 stress-controlled rotational rheometer (Guyancourt, France). All experiments in extension were performed at 180 °C. For elongational viscosity measurements, the samples were prepared by compression molding at 180 °C into the sheet shape of 1 mm. The test specimens were cut in a width of 10 and the length of 25 mm. Rectangular plates were clamped between the two counter-rotating wind-up drums. The sample width w(t) was recorded *versus* strains to confirm the linearity and thus the uniform elongation. Different samples were elongated in the melt up to very large strains. The uniaxial extensional measurements were carried out at constant strain rates from 10^{-3} to 20 s^{-1}. Therefore, the duration of tests varies from 0.19 to 38 s. The test chamber was maintained by dry nitrogen to avoid the degradation of samples. The samples were allowed to relax before each experiment to ensure that the samples were stress-free. The maximum Hencky strain was set at 3.8 by applying a given angular velocity to turn the dual wind-up drums. Most importantly, the reproducibility of the results was examined by repeating the measurements on three different specimens for each sample.

The following equation was used to calculate the elongational viscosity of molten samples in steady extension:

$$\eta_E^+(t) = \frac{T}{2R\dot{\varepsilon}_H A_0 \left(\frac{\rho_S}{\rho_M}\right)^{2/3} \exp(-\dot{\varepsilon}_H t)} \quad (1)$$

where T is the torque, R is the drum radius, A_0 is the initial area of the sample measured in the solid state, and t is the time data. The density of PLA in solid state, ρ_S, was considered 1.25 g/cm^3 and the

value for PLA melt at 180 °C, ρ_M, was 1.05 g/cm^3. Finally, the elongational viscosity of the neat and branched PBAT was hardly measured due to sagging effects prior or during the measurement. All the results shown in this paper were obtained in reproducible experiments.

Because the sample's cross-section becomes reduced during stretching, a video recorder was used to monitor this variation. The sample's section should decrease exponentially with the time when the strain rate is kept constant. For all the rate strain deformations with the Sentmanat Extensional Rheometer Generation 2, SER-G2 geometry, we experimentally validated that the strain rate was constant, thanks to a camera installed in the oven enabling to measure the real dimensions of the sample. Monitoring of the section rendered it possible to check for a constant strain rate and to determine the real strain rate applied to the polymer.

2.5.4. Start-up Shear Experiments (Transient Step Shear Rate Experiments)

The experiments were carried out in the same Discovery Hybrid Rheometer DHR-2 stress controlled rheometer using parallel-disk geometry. In this case, strain rate is commanded to increase instantaneously at time zero and the transient shear stress is recorded over time. The envelope $3\eta_0^+(t)$ in uniaxial elongation measurements has been plotted according to the experiments with 0.01 s^{-1} as a start up shear rate.

2.6. Non-Isothermal Characterization

The thermal properties of neat and processed PLA, PBAT and their blends were investigated with the help of a differential scanning calorimeter Q10 DSC (TA Instruments). The DSC cell was constantly purged with nitrogen at a flow rate of 50 mL/min. A set of heating/cooling ramps was carried out following a three step process; the samples were heated to 200 °C at 10 °C/min. The crystallinity was calculated according to the Equation (2):

$$X_c(\%) = \frac{\Delta H_m - \Delta H_{cc}}{\Delta H_{m\infty}} \times (1/w) \times 100 \quad (2)$$

where ΔH_m is the melt enthalpy; ΔH_{cc} is the cold crystallization enthalpy; $\Delta H_{m\infty}$ is theoretical specific enthalpy of fusion of the perfect crystal. It was taken as 93 J/g for PLA. It represents the. W is weight percentage of PLA in the blend.

2.7. Thermo-Mechanical Properties

The investigation of the thermo-mechanical properties was conducted through dynamic mechanical thermal analysis (DMTA) performed on a Rheometer Solids Analyser RSA II (TA instruments). Oscillating tensile-compressions tests under a strain of 0.01% at a fixed oscillatory frequency of 1 Hz were performed during temperature sweeps from −80 up to 110 °C at a rate of 3 °C/min.

3. Results and Discussion

3.1. Interfacial Tension Measurements and Morphological Properties

Before addressing the elongation properties, it would be wise to note that the interfacial properties of PLA–PBAT blends are modified with the incorporation of Joncryl.

On the one hand, the interfacial tension "α" has been measured from the deformed drop retraction method (DDRM) according to Taylor model given in Equation (3):

$$D = D^{\circ}\exp-\left\{\frac{40(p+1)}{(2p+3)(19p+16)}\frac{\alpha}{\eta_m R^{\circ}}t\right\} = D^{\circ}\exp\left\{-\frac{t}{\tau_d}\right\} = \frac{L-B}{L+B} \quad (3)$$

Here, D is the drop deformation parameter defined as $D = (L - B)/L + B$, and L and B are the major and minor axes of the ellipsoid drop, respectively. $D°$ is the initial deformation parameter, p is the viscosity ratio of the dispersed to the matrix phase, α is the interfacial tension, η_m is the viscosity of the matrix phase, and R is the radius of the drop at the equilibrium. Plotting ln(D) *versus* (t) renders possible an estimation of the interfacial tension α from the plot's slope ($-1/\tau_d$). τ_d is the relaxation time for deformed droplet retraction. More details about the calculation method are presented in our previous paper [9].

A decrease of "α" has been observed with the incorporation of Joncryl into blends, as plotted in Figure 3, highlighting once again the role of Joncryl as a compatibilizer. Therefore, the coexistence of chain extension/branching chains coupled to the PLA–Joncryl–PBAT copolymer formation had to be taken into account when studying such blends.

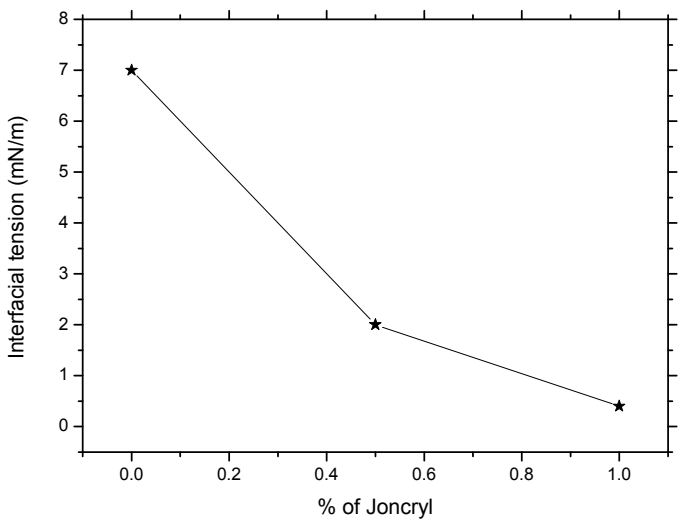

Figure 3. Evolution of the interfacial tension given by DDRM as a function of the Joncryl amount into PLA–PBAT blends.

Besides, a significant change on both deformation mechanism and break-up conditions has been elucidated, as shown in Figure 4.

On the other hand, according to SEM and TEM micrographs (see Figure 5a,b), the addition of Joncryl leads to a reduction of the average size of the dispersed PBAT phase. The ultimate volume average size was reduced from 0.25 μm for the uncompatibilized blends to 0.07 μm for the modified blend with 0.7 wt% of Joncryl. This drastic decrease could be generated from a decrease of the

mobility of the interface which slowed down the coalescence rate, related to the formation of the copolymer at the interface.

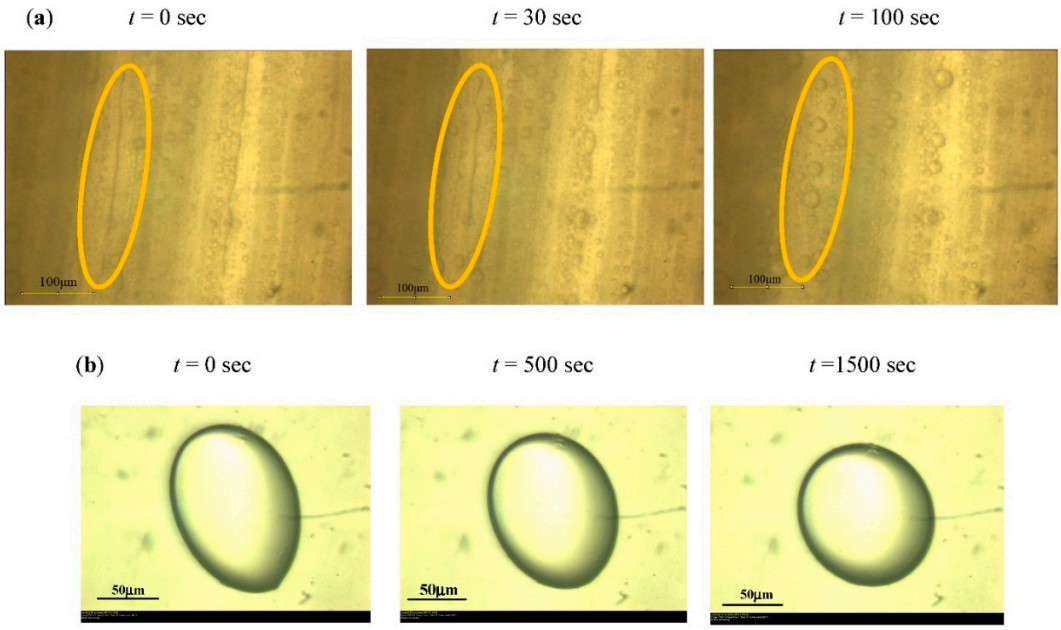

Figure 4. Examples of illustrations of the ellipsoid drop retraction, immersed in a fluid matrix at 180 °C of (**a**) uncompatibilized and (**b**) compatibilized PLA–PBAT blends. The measurement time (in second) is noted on each micrograph.

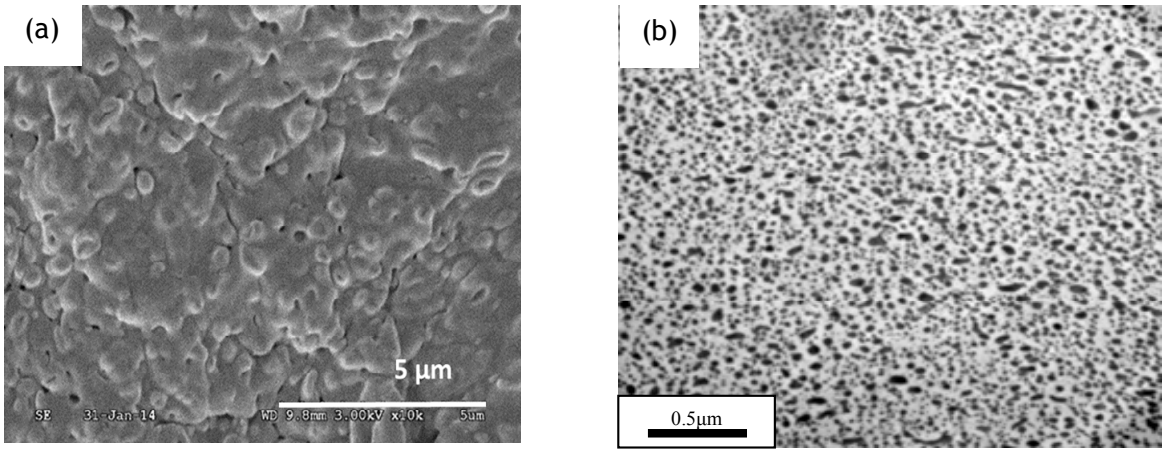

Figure 5. Examples of (**a**) SEM micrograph of PLA–PBAT (80–20) blends; Volume average diameter (D_v) = 0.25 µm and (**b**) TEM micrograph of PLA–PBAT–Joncryl (80–20–0.7); D_v = 0.07 µm.

3.2. Linear Viscoelastic and Shear Capillary Flow Properties of Neat and Modified PLA, PBAT Polymers and Their Respective Blends

Shear rheological properties of the neat PLA, PBAT polymers and their stable blends (up to reaction completion) were measured and compared in terms of dynamic viscosity modulus *versus* angular frequency as shown in Figure 6.

From Figure 6a,b, a significant increase of the complex viscosity, η*, in the low frequency region, is firstly observed with the addition of Joncryl into both PLA and PBAT. This evolution can be analyzed by the chemical reaction which can happen between each polymer with the chain extender. In fact, since Joncryl has multiple reactive end groups, several polymer chains could be chemically bounded with one Joncryl molecule. In this way, a chain extended and branched structure could be developed [5]. Secondly, a pronounced shear thinning behavior was detected. An increase of the long chain branching amount, a broadening of the molar mass distribution and a shift of the chains relaxation time for both PLA and PBAT polymers to higher values were resulted, as already demonstrated in our previous paper [5]. The modified PLA and PBAT exhibited thus a typical feature of a mixture of linear and randomly branched polymers.

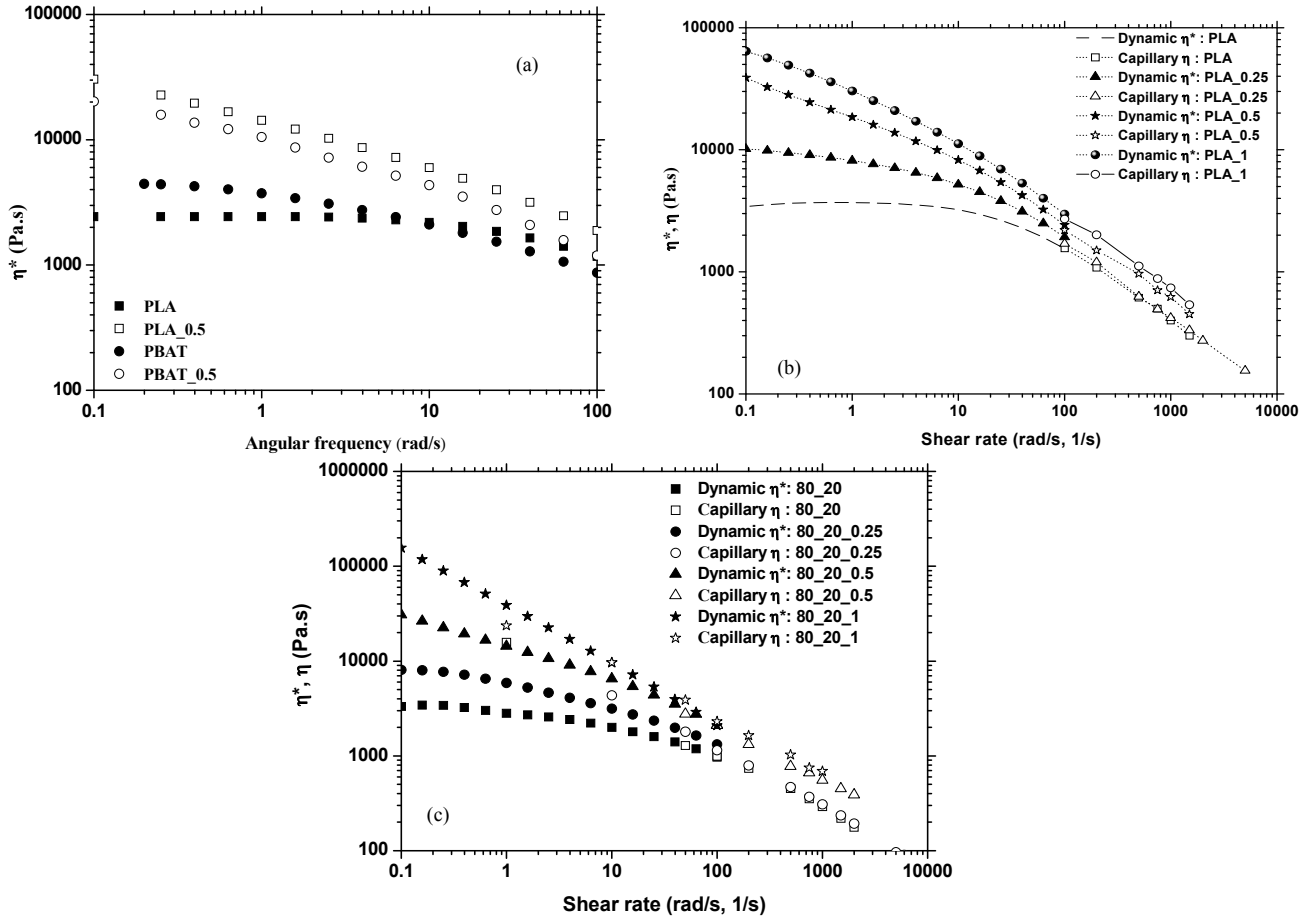

Figure 6. (**a**) Complex viscosity modulus *versus* angular frequency for neat and modified PLA and PBAT at 180 °C; (**b**) Validity of Cox–Merz rule: Dynamic viscosity modulus and shear viscosity *vs.* angular frequency (rad/s), shear rate (1/s) for the unmodified and modified PLA, PBAT polymers; (**c**) and for the uncompatibilized and compatibilized PLA–PBAT blends (Full symbol: Dynamic rheology/Open symbol: capillary rheology).

From Figure 6c, the results show that the shear viscosity and the shear-thinning tendency become stronger with increasing Joncryl content into blends. According to Figure 6b,c, the Cox–Merz rule works fairly well with neat polymers into the shear thinning region but still shows slightly deviation for the

modified polymers and their blends. The polydispersity and the heterogeneity explain this deviation from the rule [12–22]. By this way, the elongation properties during processing can ben also influenced.

3.3. Elongation Properties of Neat and Modified PLA, PBAT Polymers and Their Respective Stable Blends

Our challenge is thus to make this process stable in order to obtain stable films at higher BUR/TUR couples. To achieve this objective; a proper correlation between melt shear and extensional rheological properties should be a suitable tool to get a better handle of this process. It is well accepted that the simple shear data cannot provide direct relations with blowing extrusion flows because they only reflect the linear viscoelastic part of the material behavior. For this reason; uniaxial elongation rheology is complementary to the shear data as they capture the non-linear aspects of the melt flow and are not very far from the actual material deformation.

3.3.1. Indirect Method of Determining the Elongation Viscosity—Cogswell Elongation Viscosity

Using the capillary rheological data of our different samples, the elongational viscosity η_E, was evaluated by the indirect Cogswell method. It is a simple rheological technique based on the entrance pressure drop method and based on the relationship between the elongational viscosity and the pressure at the die governed by the melt elasticity [21]. Figure 7 depicts an example of the evolution of the η_E after Bagley correction for the modified PLA with three different amounts of Joncryl (up to 1% by weight) at a fixed elongation rate (30 s^{-1}). It can be seen that the η_e is increasing with the incorporation of Joncryl. The enhancement of melt strengthening of the modified PLA, as already discussed in detail [5], was thus confirmed by the drastic increase of the elongational viscosity.

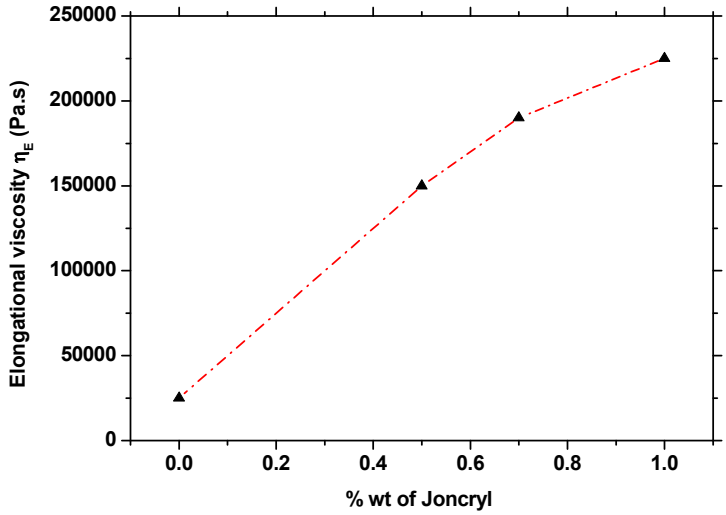

Figure 7. Example of the evolution of the elongational viscosity at 180 °C given by Cogswell method *versus* the Joncryl® amount of the modified PLA at 30 s^{-1}.

For PLA–PBAT blends, the elongational viscosity determined by Cogswell is increasing with the amount of Joncryl. This increase is related to the reaction between PLA, PBAT polymers and the multifunctional epoxide as presented in Figure 8. Therefore, an improvement of the blown film extrusion ability can be expected.

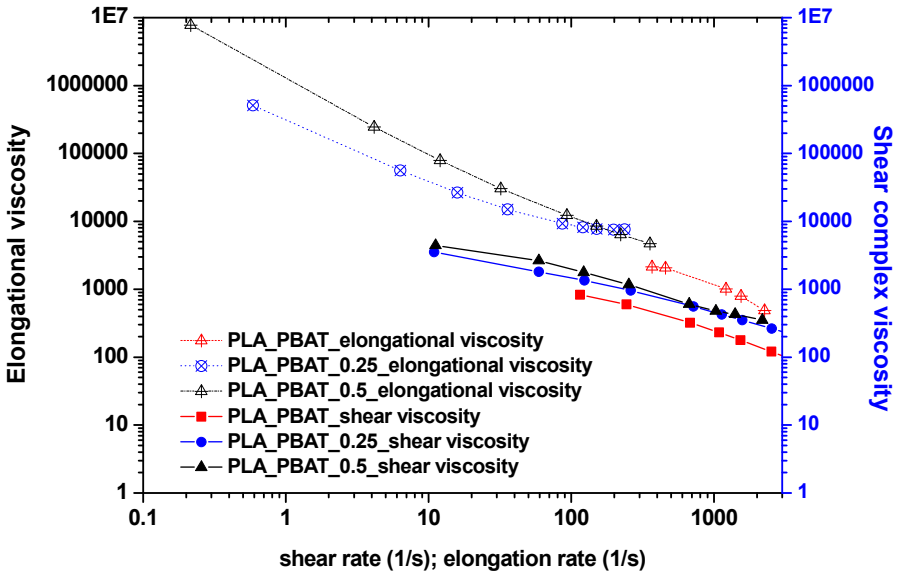

Figure 8. Elongational and shear viscosities *versus* elongation (and shear) rate for the non compatibilized and compatibilized PLA–PBAT blend at 180 °C.

In the next section, the transient elongational viscosity of the samples will be quantified more accurately.

3.3.2. Uniaxial Extensional Experiments

Neat PLA and PBAT Polymers

Figure 9 shows double logarithmic plots of the transient elongation viscosity η_E *versus* time *t*, observed for both PLA and PBAT polymers at 180 °C. Uniaxial elongation experiments were conducted at various shear rates ranging from 0.1 to 20 s^{-1}. The extensional data are superposed well with the linear viscoelastic envelope (LVE) ($3\eta_0^+(t)$) at lower times. This indicates that the Trouton ratio ($T_R = \eta_e/\eta_0$) is equal to 3, the limiting case of Newtonian polymer. For PLA, the absence of a deviation could be explained by the Brownian motion where macromolecules tend to return to their equilibrium configuration after being subjected to deformations. The PLA and PBAT polymers did not exhibit any strain-hardening up to 1 s^{-1}. This is the ordinary behavior of the linear polymers which is called strain-softening phenomena, as discussed by Liu *et al.* [14]. The presence of free volume within polymer chains could hinder the formation of entanglements through reduced contact surface and ineffective overlapping. Consequently, the linear chains are being free from any branch points and are not prevented from slipping over each other. The absence of strain hardening behavior of both PLA and PBAT could confirm that they are not favorable for blown film application. However, at high values of the Hencky strain rate (>5 s^{-1}), it was speculated that an apparent strain hardening was observed. The Trouton rule does not hold; at longer times, the η_e^+ deviates from the linear viscoelastic behavior. The observed increase could be due to shorter overlapping time of macromolecules during elongational flow. Thus, the occurrence of the strain hardening behavior of linear PLA has been reported in few studies and might be due to its stereo-regularity [15–27]. In fact, the stereo-regularity of high L-content PLA (98% of L-content in our case) may allow them to form a range of structures

when stretched, where helical conformations may form in the melt as a precursor to strain-induced crystallization. This behavior was not observed in our previous work with other grade of PLA.

For PBAT, care should be taken when analyzing the results since (i) it is not strong enough to be tested at 180 °C and (ii) Its higher sagging during experiments. The higher molar masses and the presence of rigid chains with phenyl component could explain the apparent strain hardening observed at high strain rate.

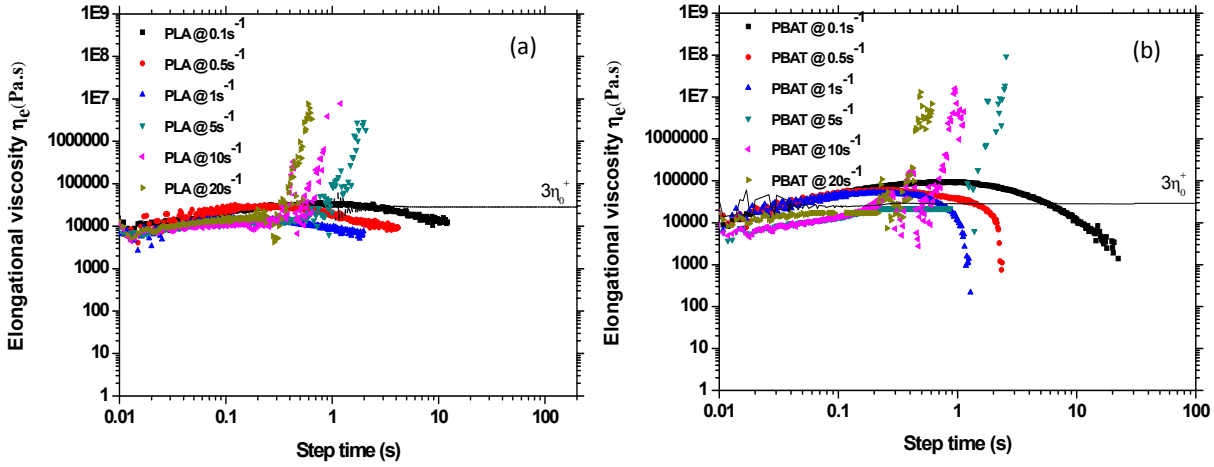

Figure 9. Start-up elongation viscosity *versus* step time at 180°C for the neat (**a**) PLA polymers and (**b**) PBAT polymers at different elongation rates.

Modified PLA System

Figure 10 displays the transient elongational viscosities for the branched PLA. For the clarity purpose, only the results with 0.7 wt% of Joncryl will be shown thereafter. In all cases, the extensional viscosities raise above the linear viscoelastic envelope. A distinguished strain hardening is observed even at low strain rates whereas for linear PLA no strain hardening has been reported. It increases with increasing strain rate; in the early stage, η_e gradually increases with time but is almost independent of the elongation rates. After a certain time *t*, elongation viscosity shows a rapid upward deviation (which correspond to higher Trouton ratio) due to the resistance caused by the branches intermingled with the main chains of the polymer. Thus, the modified polymer resisted up to the elongational deformation without failure for the complete test durations. Considering the wide polydispersity for the modified PLA, this gives rise to the assumption that the effect of the branching structure on the strain hardening dominates [28,29]. Depending on the number of branches and molecular weight, entanglement density may be increased or decreased by branching. In this study, based on the data presented in the paper and the observed positive deviation, entanglement density was increased. Moreover, the strain hardening is not only accorded to the presence of branch which they reduce the rate of chain disentanglement. Indeed, some gripping forces can happen depending of branch density and length. The literature suggests that the strain-hardening is exhibited when the rate of the deformation considerably exceeds the rate of molecular relaxation [30]. The longest relaxation time was obtained by analyzing the linear viscoelastic data in terms of its discrete relaxation spectrum, as presented in our previous paper [11]. As the longest relaxation time of a modified PLA is larger than the solicitation time, strain hardening effects are expected.

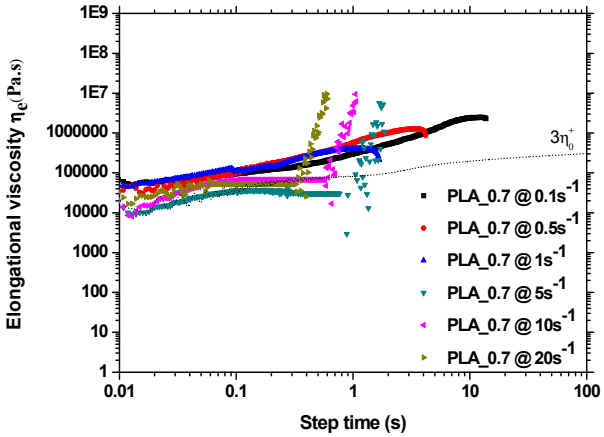

Figure 10. Start-up elongation viscosity *versus* step time for the modified PLA with 0.7 wt% of Joncryl at different elongation rates at 180 °C.

PLA-PBAT Blends

Elongational flow properties of PLA/PBAT 80–20 blends are given in Figure 11. The results illustrate that their behavior is more dominated by the PLA matrix. At a strain rate less than 1 s^{-1}, the extensional viscosity of the uncompatibilized blends tends to hold the Trouton rule. The envelope of compatibilized PLA–PBAT blends is over 10,000 Pa·s in comparison of non-compatibilized systems. Therefore, an increase of the elongational viscosity was observed for the whole range of elongation rates for the compatibilized blends. The indications are that the stronger the interface, the highest the elongational deformation. At high elongation rates, the strain hardening was expected as is the case of neat polymers. It could be attributed to the occurrence of trans-esterification reactions in the uncompatibilized PLA–PBAT blend and to the strong interfacial adhesion in the compatibilized PLA–PBAT–Joncryl blend [9]. Like Cogswell indirect results (Figure 8), the addition of Joncryl improve the elongational behavior of the blends.

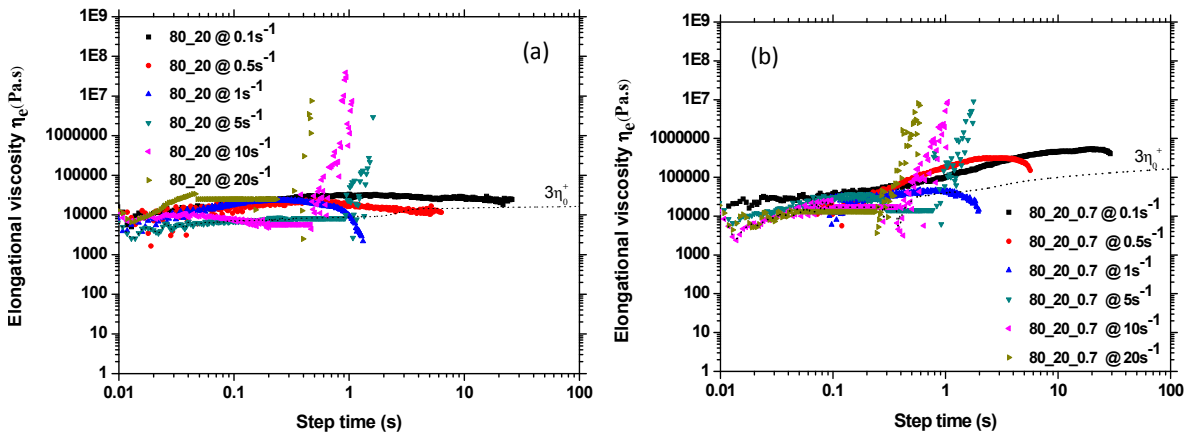

Figure 11. Elongation viscosity *versus* step time (*t*) 180 °C for the (**a**) uncompatibilized and (**b**) compatibilized PLA–PBAT blends at different elongation rates.

According to the transient elongational behavior of the uncompatibilized and compatibilized PLA–PBAT blends presented in the previous section, the measured engineering stress for each PLA and its blends is firstly plotted in Figure 12 according to Equation (4):

$$\sigma_{engineering} = \frac{F_{elongation}}{S} = \eta_{elongation} \times \dot{\varepsilon} \quad (4)$$

where $F_{elongation}$ is the elongational force and S is the section of the specimen.

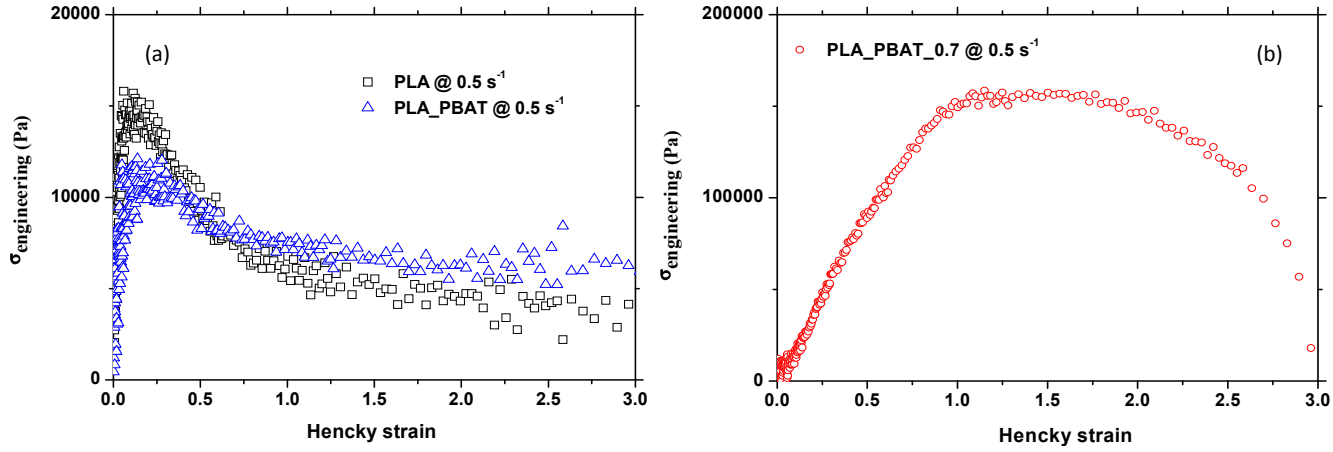

Figure 12. Example of engineering stress evolution at 0.5 s^{-1} at 180 °C for (**a**) PLA and its uncompatibilized blend and (**b**) its compatibilized blend.

It was clearly observed that the neat PLA and its uncompatibilized blend break at complete sample failure at 0.5 Hencky. Hence, a pronounced decrease of the engineering stress is observed.

However, the compatibilized blend breaks at around 2 of strain Hencky deformation amplitude. Note that it takes more stress, or more elongational force, to extend them at a constant strain rate, for which the interfacial adhesion between matrix and dispersed phase is strong. For instance, at 0.5 s^{-1}, the force is 10 times higher than for the uncompatibilized counterpart.

3.4. Application to Blown Film Extrusion: Investigation of the Stability Processing of Neat/Modified Polymers and Their Blends

3.4.1. Stability Processing of Neat PLA and PBAT Polymers

The instability defects in blown film were firstly reported by Han and co-workers [23,24]. They observed that depending on the processing parameters and the rheological properties of materials, different instabilities can appeared, *i.e.*, lowering the extrusion temperature stabilized the blown bubble for high density polyethylene (HDPE) and low density polyethylene (LDPE). Some other authors have more extensively discussed the instabilities during blown film processing [25,26].

In our case, the study of the stability of the process was conducted by establishing the stability map (BUR *vs.* TUR). Thereby, these two main parameters were changed and bubble stability or instability was observed. The BUR(s) values have changed according to air flow inflated into the die. The TUR(s) have changed based on the variation of the chill roll velocity and the melt flow was kept

constant. The process was considered as stable since no defect appeared for a given BUR–TUR couple during at least 10 min.

PLA shows a limited blowing ability according to its stability map plotted in Figure 13. Any stable blown film has been obtained neither at lower BUR–TUR couple nor at higher ones. The map presents unstable points related to different instabilities including (i) draw resonance; (ii) helical instability; (iii) frost line oscillation; (iv) breathing; (v) dancing and; (vi) bubble sag. Moreover, PBAT has no ability to be blown. Its stability map cannot be plotted due to sagging problem. The poor shear and elongation properties of PLA and PBAT could explain their inadaptability to the blown film process.

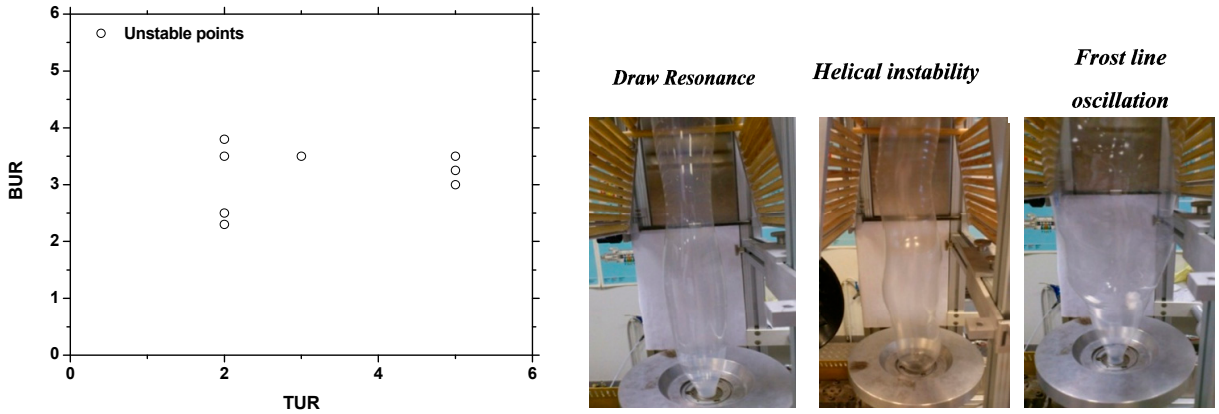

(**a**) (**b**)

Figure 13. Stability map (BUR *versus* TUR) of neat PLA at 180°C (**a**). Various instabilities observed (**b**).

3.4.2. Stability Processing of Chain Extended/Branched PLA Polymers

We have shown that the structural modification of PLA (PLA with Joncryl) leads to an increase in elongational viscosity by 6 orders of magnitude at 0.1 s. This is the property that mostly determines the bubble stability and ease of processing as presented in Figure 14. The Blow-Up Ratio (BUR on *y* axis) values rose from 2.5 to 7. Large bubbles were formed. Stable bubbles were obtained at high Take-Up Ratio (TUR on *x* axis) of 6. The occurred instabilities are less chaotic compared to pure PLA.

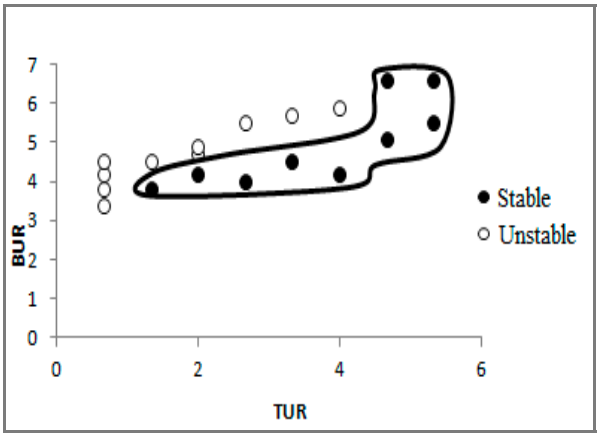

(**a**)

Figure 14. *Cont.*

(**b**) (**c**)

Figure 14. (**a**) Stability maps (BUR *versus* TUR) of modified PLA with 0.7 wt% of Joncryl. Comparison of the bubble shape between (**b**) PLA and (**c**) PLA–0.7; Unlike PLA, large and stable bubbles were obtained with the incorporation of Joncryl.

3.4.3. Stability Processing of PLA–PBAT Blends

The stability map of the uncompatibilized blend is established and presented in Figure 15. The results show that the incorporation of PBAT into PLA matrix leads to an enlargement of the stability domain. BUR raises to 3.5. Three types of defects have been detected which are breathing, draw resonance and dancing. But, breathing instability remains the main occurred defect. It is important to note that the PLA–PBAT blends present a more stable region for higher TUR compared to the modified PLA polymers. Self-compatibilization behavior between PLA and PBAT according to some trans-esterification reaction can occur. Indeed, a bit increase of its elongation properties was noted in the previous section and could explain a stable blown behavior. However, it retracts when the biaxial stress is suppressed. Therefore, the obtained bubbles are not very large and BUR is lower compared to the modified PLA (PLA–Joncryl) film which reach 7 but at not at a higher TUR.

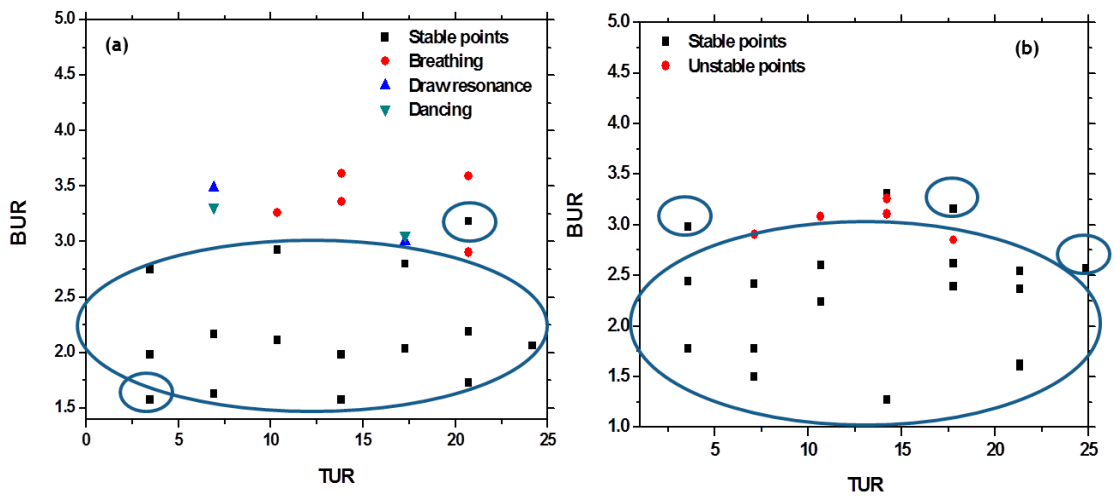

Figure 15. Stability maps of the (**a**) uncompatibilized PLA-PBAT blends and (**b**) compatibilized PLA–PBAT blends with 0.7 wt% of Joncryl.

With the incorporation of Joncryl ADR®, the breathing instability zone is reduced and the draw resonance instability is eliminated (Figure 16).

(**a**) (**b**) (**c**)

Figure 16. Comparison of the bubble shape between (**a**) PLA; (**b**) PLA–PBAT and (**c**) PLA–PBAT–0.7.

Once can conclude that Joncryl helps process stabilization at lower and higher TUR which ensure an achievement of high BUR values. Meanwhile, the addition of Joncryl leads to an increase in engineering stress and elongational viscosity according to the stronger interfacial cohesion between matrix and dispersed phase. This is the main difference with the uncompatibilized systems. Moreover, a new zone of stable bubble can be obtained with higher TUR values (25 of amplitude) and BUR reaching 3.5. The compatibilization effects of the Joncryl play a real role to eliminating dancing and draw resonance defects according to the induced higher elongation properties at great strain Hencky deformation amplitude.

3.5. Thermo-Mechanical and Crystalline Properties of the Blown Films

Table 2 includes the thermal transitions and crystalline properties of our studied systems. It is worthy concluded that the blowing extrusion altered the crystalline properties of neat and modified PLA due to the orientation of polymer chains upon biaxial strain. The crystallinity level increases from 4% to 6.5% and from 5.5% to 13% after blowing for neat and modified PLA, respectively. A depression of the cold crystallization temperature, T_{cc} is also observed. It should be pointed out that the glass transition temperature, occurring within the 60–65 °C range, is nearly unaffected by the processing.

The incorporation of PBAT leads to a significant increase of the crystallinity of the PLA–PBAT blown film, explaining its ability to be blown and to be crystallizing. However, with the addition of Joncryl, the crystallinity level increases slightly. The development of crystalline structure in modified PLA–PBAT blends is effectively hindered. This can be related to the higher branching density, as demonstrated for PET [31], despite it exhibits a slightly increase of the cold crystallization compared to the unmodified one.

Table 2. Thermal parameters and crystallinity values of unblown and blown systems.

Films	T_g (°C)	T_{cc} (°C)	ΔH_{cc} (J/g)	T_m (°C)	ΔH_m (J/g)	X_c (%)
PLA before blowing	60	115	24	170	25	4
PLA–0.7 before blowing	59	111	33	169	38	5.5
80–20 before blowing	−31/62	98	20.5	169	28	11
80–20–0.7 before blowing	−30/62	108	20	167.5	25	7
PLA after blowing	61.5	110	27	170	33	6.5
PLA–0.7 after blowing	63	98	28	170	40	13
80–20 after blowing	−29/64	103	11	171	29	24
80–20–0.7 after blowing	−29/63	95	13	169	19	9

Representative curves of DMTA recording tanδ and log*E*' for the neat and modified blown PLA films are shown in Figure 17. The solid-state rheological properties of PLA typically show in its glassy state, a storage modulus (*E*') of about 3 × 10^9 Pa. As the sample is heated above T_α, a sharp drop in modulus occurs between 55 and 75 °C and *E*' decreases to 5 × 10^6 Pa by softening the film. This region is accompanied by a maximum peak of tanδ of about 65 °C, which corresponds to the α-relaxation of PLA. The obtained data regarding the relaxation α of PLA and modified PLA corroborate those in the literature [32,33].

The storage modulus then increases at a temperature around 83–85 °C. This recovery is attributed to the cold crystallization of the PLA chains, being higher with increasing the crystallinity of PLA when comparing with DSC thermograms.

From Figure 17a, we can conclude that the curve of PLA with Joncyl almost has the same shape as the neat PLA below the melting temperature. An increase of the storage modulus (*E*') below the α-relaxation is observed. A strain-induced crystallization may had occurred upon biaxial blowing where Joncryl acts as precursor of new nucleation sites, enhancing the growth of the crystalline phase. Moreover, the tanδ curves is nearly unaffected by the structural changes induced upon reaction with the chain extender indicating that the Joncryl ADR® did not act as a plasticizer agent.

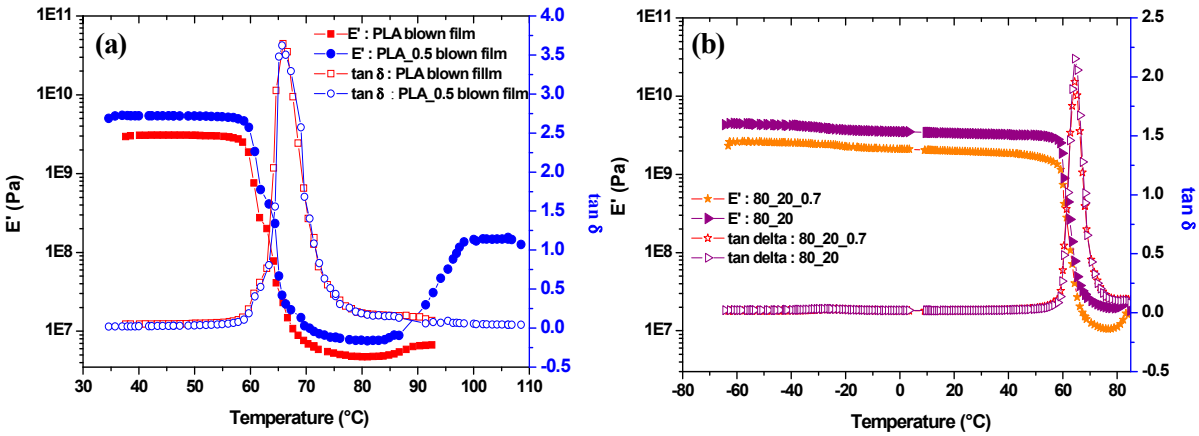

Figure 17. Storage modulus and loss factor evolution *versus* temperature for (**a**) PLA and PLA–0.7 and (**b**) PLA–PBAT blends.

The thermo-mechanical behavior of the modified and unmodified PLA–PBAT blends showed that the high storage modulus is observed for the PLA–PBAT blend compared to its modified counterpart.

This is probably to the high obtained crystallinity upon blowing as shown in Table 2. In both cases, an increase of the storage modulus is observed at around 80 °C, highlighting the cold crystallization behavior of PLA. Such evolution indicates that the prepared blown films are semi-crystalline, as also confirmed by DSC data.

At low temperature relaxation (−27 °C) and for low contents of PBAT, the PBAT α-relaxation is not clearly visible. Moreover, the reactive agent (Joncryl) did not affect the tanδ of PLA–PBAT blends. The loss factor peak of blends (tanδ = 2.2) showed a decreased magnitude of tanδ in comparison to virgin PLA (tanδ = 3.7). This behavior is mainly due to the rubbery phase of PBAT which is well dispersed in PLA matrix.

4. Conclusions

Two main routes has been investigated in the present work: (i) a structural modification through chain extension and branching mechanisms by adding a reactive multifunctional epoxide (Joncryl) and (ii) blending with PBAT in presence (or nor) of this reactive agent. Through this paper, structure–processing–properties relationships have been addressed. Several conclusions can be derived.

On the one hand, both PLA and PBAT are not able to be blown at lower Hencky strain rate (>1 s^{-1}) since their respective elongational properties are weak. For PBAT, care should be taken when analyzing the results since it is not strong enough to be tested at 180 °C.

On the other hand, the change of the molecular structure of PLA by incorporating 0.7 wt% of Joncryl resulted in significant shear and elongational behavior (higher shear and elongation viscosity, presence of strain hardening behavior even at lower strain rates). Consequently, its ability to blowing was enhanced. Stables bubbles with higher BUR and TUR were obtained.

For PLA–PBAT blends, the effect of Joncryl on the shear and elongation rheology, morphological, and interfacial properties of the blends was investigated. The role of Joncryl as a compatibilizer was highlighted thanks to scanning and transmission electron microscopy (SEM and TEM) observations and the DDRM.

For the first time, the elongational measurements of the non-compatibilized and compatibilized PLA–PBAT blends were assessed. The results showed that the elongational behavior has been governed by the matrix. A strain-hardening was thus expected. In all, the incorporation of PBAT into PLA matrix leads to an enlargement of the stability domain.

The incorporation of PBAT into PLA matrix leads to an enlargement of the stability domain according to some self-compatibilization behavior (trans-esterification reaction can occur).

Furthermore, the addition of Joncryl leads to an increase in engineering stress and elongational viscosity according to the stronger interfacial cohesion between matrix and dispersed phase. A reduction of the instability zone and a new zone of stability was obtained. The draw resonance and the dancing defects are totally eliminated. Moreover, higher values of BUR have been reached although TUR is quite higher.

Finally, it has been demonstrated that the blown film extrusion process leads to semi-crystalline films with improved thermo-mechanical properties.

Acknowledgments

The authors gratefully acknowledge the 'DGCIS' (Direction Générale de la Compétitivité de l'Industrie et des Services) for the Financial support. The authors also express their appreciation to the reviewers for their meticulous review and assessment of this work.

Author Contributions

The authors contributed equally to this work. They all participated to the writing of the present manuscript. Racha Al-Itry performed the overall experimental work as a PhD Student in INSA de Lyon, France. The settings up of the experimental protocols as well as the interpretation of the obtained results were performed under the supervision of khalid Lamnawar and Abderrahim Maazouz.

Conflicts of Interest

The authors declare no conflict of interest.

References

1. Kanai, T.; Campbell, G.A. *Film Processing*; Carl Hanser Verlag: Munich, Germany, 1999.
2. Lim, L.T.; Auras, R.; Rubino, M. Processing technologies for poly (lactic acid). *Progr. Polym. Sci.* **2008**, *33*, 820–852.
3. Jung, H.W.; Hyun, J.C. Instabilities in extensional deformation polymer processing. *Rheol. Rev.* **2006**, *2006*, 131–164.
4. Arraiza, A.L.; Sarasua, J.R.; Verdu, J.; Colin, X. Rheological behavior and modeling of thermal degradation of poly(ε-caprolactone) and poly(L-lactide). *Int. Polym. Process. XXII* **2007**, *22*, 389–394.
5. Al-Itry, R.; Lamnawar, K.; Maazouz, A. Improvement of thermal stability, rheological and mechanical properties of PLA, PBAT and their blends by reactive extrusion with functionalized epoxy. *Polym. Degrad. Stab.* **2012**, *97*, 1898–1914.
6. Baird, D.J. The role of extensional rheology in polymer processing. *Korea-Aust. Rheol. J.* **1999**, *11*, 305–311.
7. Mihai, M.; Huneault, M.; Favis, B.D. Rheology and extrusion foaming of chain-branched poly(lactic acid). *Polym. Eng. Sci.* **2010**, *50*, 629–642.
8. Japon, S.; Luciani, A.; Nguyen, Q.T.; Leterrier, Y.; Manson, J.A.E. Molecular characterization and rheological properties of modified poly(ethylene terephthalate) obtained by reactive extrusion. *Polym. Eng. Sci.* **2001**, *41*, 1299–1309.
9. Al-Itry, R.; Lamnawar, K.; Maazouz, A. Rheological, morphological, and interfacial properties of compatibilized PLA/PBAT blends. *Rheol. Acta* **2014**, *53*, 501–517.
10. La Mantia, F.P.; Valenza, A.; Scargiali, F. Non isothermal elongational behavior of blends with liquid crystalline polymers. *Polym. Eng. Sci.* **1994**, *34*, 799–803.
11. Al-Itry, R.; Lamnawar, K.; Maazouz, A. Reactive extrusion of PLA, PBAT with a multi-functional epoxide: Physico-chemical and rheological properties. *Eur. Polym. J.* **2014**, *58*, 90–102.

12. Corre, Y.M.; Duchet, J.; Maazouz, A.; Reignier, J. Melt strengthening of poly (lactic acid) through reactive extrusion with epoxy-functionalized chains. *Rheol. Acta* **2011**, *50*, 612–629.
13. Mallet, B.; Lamnawar, K.; Maazouz, A. Improvement of blown film extrusion, of poly (lactic acid): Structure-processing properties relationships. *Polym. Eng. Sci.* **2014**, *54*, 840–857.
14. Liu, J.; Lou, L.; Yu, W.; Liao, R.; Li, R.; Zhou, C. Long chain branching polylactide: Structures and properties. *Polymer* **2010**, *51*, 5186–5197.
15. Palade, L.L.; Lehermeier, H.J.; Dorgan, J.R. Melt rheology of high L-content poly(lactic sacid). *Macromolecules* **2001**, *34*, 1384–1390.
16. Corre, Y.M.; Maazouz, A.; Duchet, J.; Reignier, J. Batch foaming of chain extended PLA with supercritical CO_2: Influence of the rheological properties and the process parameters on the cellular structure. *J. Supercrit. Fluids* **2001**, *58*, 177–188.
17. Zhu, W.L.; Wang, J.; Park, C.B.; Pop-Iliev, R.; Randall, J. Effects of chain branching on the foamability of polylactide. In Proceedings of 67th Annual Technical Conference of the Society of Plastics Engineers (SPE-ANTEC), Chicago, IL, USA, 22–24 June 2009; Volume 1, pp. 41–45.
18. Eslami, H.; Kamal, M.R. Effect of a chain extender on the rheological and mechanical properties of biodegradable poly(lactic acid)/poly(butylene succinate-*co*-adipate) blends. *J. Appl. Polym. Sci.* **2013**, *129*, 2418–2428.
19. Kim, Y.M.; Park, J.K. Effect of short chain branching on the blown film properties of linear low density polyethylene. *J. Appl. Polym. Sci.* **1996**, *61*, 2315–2324.
20. Majumder, K.K.; Hobbs, G.; Bhattacharya, S.N. Molecular, rheological, and crystalline properties of low-density polyethylene in blown film extrusion. *Polym. Eng. Sci.* **2007**, *47*, 1983–1991.
21. Cogswell, F.N. Converging flow of polymer melts in extrusion dies. *Polym. Eng. Sci.* **1972**, *12*, 64–73.
22. Lehermeier, H.J.; Dorgan, J.R. Melt rheology of poly (lactic acid): Consequences of blending chain architectures. *Polym. Eng. Sci.* **2001**, *41*, 2172–2184.
23. Han, C.D.; Park, J.Y. Studies on blown film extrusion. III. Bubble instability. *J. Appl. Polym. Sci.* **1975**, *19*, 3291–3297.
24. Han, C.D.; Shetty, R. Flow instability in tubular film blowing. 1. Experimental study. *Ind. Eng. Chem. Fundam.* **1977**, *16*, 49–56.
25. Kanai, T.; White, J.L. Kinematics, dynamics and stability of tubular film extrusion of various polyethylenes. *Polym. Eng. Sci.* **1984**, *24*, 1185–1201.
26. Minoshima, W.; White, J.L. Instability phenomena in tubular film and melt spinning of rheological characterized high density, low density and linear low density polyethylenes. *J. Non-Newton. Fluid Mech.* **1986**, *19*, 275–302.
27. Yamane, H.; Sasai, K.; Takano, M. Poly(D-lactic acid) as a rheological modifier of poly(L-lactic acid): Shear and biaxial extensional flow behavior. *J. Rheol.* **2004**, *48*, 599–609.
28. Mekhilef, N.; Hedhli, L.; Moyses, S. Effect of rheological strain hardening on extrusion blown film of polyvinylidene fluoride. *J. Plast. Film Sheeting* **2007**, *23*, 203–219.
29. Stange, J.; Uhl, C.; Münstedt, H. Rheological behavior of blends from a linear and a long-chain branched polypropylene. *J. Rheol.* **2005**, *49*, 1059–1080.
30. Kasehagen, L.J.; Macosko, C.W. Nonlinear shear and extensional rheology of long-chain randomly branched polybutadiene. *J. Rheol.* **1998**, *42*, 1303–1327.

31. Raffa, P.; Coltelli, M.B.; Savi, S.; Bianch, S.; Castelvetro, V. Chain extension and branching of poly(ethylene terephthalate) (PET) with di- and multifunctional epoxy or isocyanate additives: An experimental and modelling study. *React. Funct. Polym.* **2012**, *72*, 50–60.
32. Henton, D.E.; Gruber, P.; Lunt, J.; Randall, J. Polylactic acid technology. In *Natural Fibers, Biopolymers, and Biocomposites*; Mohanty, A.K., Misra, M., Drzal, L.T., Eds.; Taylor & Francis: Boca Raton, FL, USA, 2005; pp. 527–577.
33. Huda, M.S.; Yasui, M.; Mohri, N.; Fujimura, T.; Kimura, Y. Dynamic mechanical properties of solution-cast poly(L-lactide) films. *Mater. Sci. Eng. A* **2002**, *333*, 98–105.

© 2015 by the authors; licensee MDPI, Basel, Switzerland. This article is an open access article distributed under the terms and conditions of the Creative Commons Attribution license (http://creativecommons.org/licenses/by/4.0/).